INJURY BIOMECHANICS RESEARCH
Proceedings of the Twenty-fourth International Workshop

An Experimental Study of Airbag-Induced Eye Injuries

Stefan M. Duma[1], Tyler A. Kress[2], David J. Porta[3], Peter G. Martin[1], Rodney J. Simmons[4], Cherie L. Alexander[2], Charles D. Woods[1]

1. University of Virginia, Automobile Safety Laboratory
2. University of Tennessee
3. Bellarmine College
4. University of Cincinnati

ABSTRACT

This paper provides the results from two series of tests intended to contribute to an increased understanding of airbag induced eye injuries. In the first series of tests, airbags were deployed onto an instrumented dummy head. Seven force transducers, each having a 2.25 cm^2 contact area, were placed on one aspect of the orbital region to evaluate the force patterns. Seven different types of airbags were used that included tethered and nontethered, light to heavy nylon weaves, and different coating types. The average maximum forces per sensor range from 15.4 N to 63.6 N, peak pressures range from 68 kPa to 282 kPa, with the upper center of the eye presenting the highest values. The second set of testing involved the deployment of several types of airbags onto thirteen unembalmed, previously frozen cadaver heads. Eyeglasses were placed on four of the test specimens. High speed video and film were used to capture the events, while ultrasound imaging, fluorescein dye testing, and dissection were the methods used to evaluate the induced injuries. The impact velocities of the airbags were recorded at the first contact location with the eye. The presence of eyeglasses seemed to provide protection because of the lack of contact between the airbag and the ocular region. Minimal ocular damage was recorded for these experiments.

INTRODUCTION

While it has been statistically shown that airbags save lives, the current design of the airbag system should be improved to minimize the minor injuries associated with its deployment (1-2). Airbag induced eye injuries, although uncommon, present a concern due to their potential for serious and permanent damage. Partial and even total blindness have been recorded in some cases (3-4).

Airbag induced eye injuries may be divided into two categories. The first stems from the mechanical aspects of the deploying airbag and includes such injuries as abrasions, vitreous hemorrhages, hyphemas, and retinal tears and detachment (5-13). Three mechanisms have been used to describe these injuries as forms of blunt ocular trauma: coup, contrecoup, and equatorial expansion (14). Coup injury is caused by direct impact that produces localized damage, while contrecoup injury occurs at tissue interfaces along the line of applied force and not necessarily in the direct vicinity of the impact. Equatorial expansion, which is widely accepted as the primary causal mechanism for retinal detachments, involves the globe compressing along the anterior-posterior axis while it expands along the perpendicular equator of this axis. As the equator of the globe expands, the retina is pulled away by a tensile force created by the fact that the inside of the eye expands slower than the outside. Corneal endothelial cell loss as a result of eyeball deformation during impact is also included in this category. In experimental tests, increased corneal endothelial cell loss has been correlated with increased airbag inflator power (15).

Individuals may be predisposed to airbag-induced eye injuries. For example, radial keratotomy, which is the technique of making small incisions in the surface of the cornea to improve sight, has been shown to decrease the strength of the cornea in rabbits by 50% over a 90 day period after surgery (16).

The second category of airbag induced eye injuries is alkaline chemical keratitis, or inflammation of the cornea, which is caused by the deposition into the eye of sodium hydroxide. In a humid environment the burning of sodium azide will produce a small amount of the very alkaline substance, sodium hydroxide. Alkaline materials are well known for their ability to produce eye injuries, and several cases have been reported as a result of deployed airbags (17-19). If detected in the early stages, this injury can be treated by flushing the eye with copious amounts of water (20).

This paper aims at better understanding the first group of injuries by examining the interaction between a deploying airbag and the eye. Two sets of experiments were performed to provide new data on this topic: airbag deployments onto an instrumented dummy head, and airbag deployments onto unembalmed and previously frozen cadaver heads.

ANATOMY - A brief review of the relevant anatomy is presented in Figure 1. The cornea is the clear membrane that makes up the anterior 1/6 of the sclera. It is comprised of five layers: epithelium (anterior layer), Bowman's membrane, substantia propria corneae, Descemets' membrane, and the endothelium (posterior layer). The endothelial cells area extremely important in that they keep the cornea clear. The posterior layer of the cornea consists of a single layer of these cells. Moreover, since they exhibit no mitotic activity, once they are dead they are not replaced and maintaining corneal clarity becomes difficult. The anterior chamber is filled with a watery fluid that is filtered and replaced hourly. The shape of the lens is controlled by the ciliary muscle in order to properly focus light on the retina. The vitreous humor, a jello-like substance

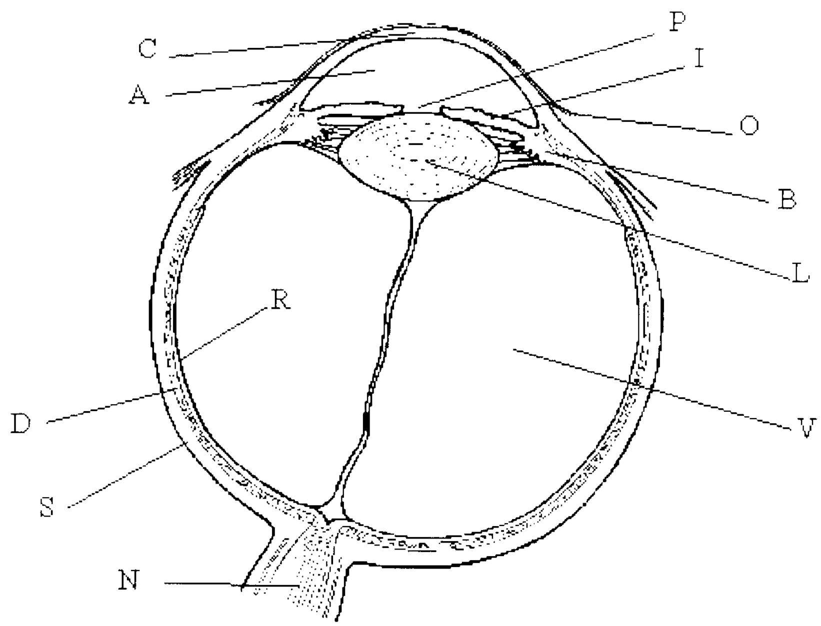

Figure 1: Important Ocular Structures
(A=anterior chamber, B=ciliary body, C=cornea, D=choroid, I=iris, L=lens,
N=optic nerve, O=conjunctiva, P=pupil, R=retina, S=sclera, V=vitreous humor)

that does not change, comprises the large volume in the center of the eye. The posterior 5/6 of the outside of the eye consists of a three layered membrane. The sclera is the outside layer which forms into the cornea anteriorly. The middle layer is the choroid, which becomes the ciliary body and iris anteriorly, and is responsible for providing the blood supply to the retina. The retina, the delicate innermost layer, is the light transducing portion of the eye.

Yamada (1970) details the biomechanical properties of the human cornea and sclera (21). He states that the ultimate tensile strength for the cornea is 3.4 MPa and shows no difference between infants and adults as well as between the sexes. The ultimate tensile strength of the sclera, which is dependent on direction, is 7.55 MPa in the equatorial direction and 4.7 MPa in the meridional direction. After approximately 20 years of age, the strength of the sclera shows no change.

EYE INJURY CASE STUDIES - The NASS database was searched for the years 1993 through 1995 for all eye injuries. The AIS ranking for eye injuries is outlined in Table 1. It should be noted that the low AIS 2 rating of eye enucleation is due to the emphasis this scale places on threat to life, and although total eye loss is debilitating, it is not life threatening. From the NASS database Figure 2 reveals the unweighted total number of people with an airbag-induced eye injury for the past 3 years, as well as the total number of recorded eye injuries from airbags recorded in these cases. As expected, the number increases each year. Theses cases are compiled from a sample of approximately 4500 cases investigated each year. For the time period examined, it is estimated that only 20% of the automobiles in use have airbags; however, by the year 2000, it is expected that over 50% of the fleet will be equipped with at least driver-side airbags. A fact that would indicate a further increase in the rate of eye injuries from airbags.

Table 1: AIS Values for Eye Injuries

AIS Value	Injury
2	Eye enucleation; Retinal Detachment; Sclera Rupture/Laceration Involving Globe
1	All Others (i.e. Corneal Abrasion, Hyphema, Conjunctiva Injury)

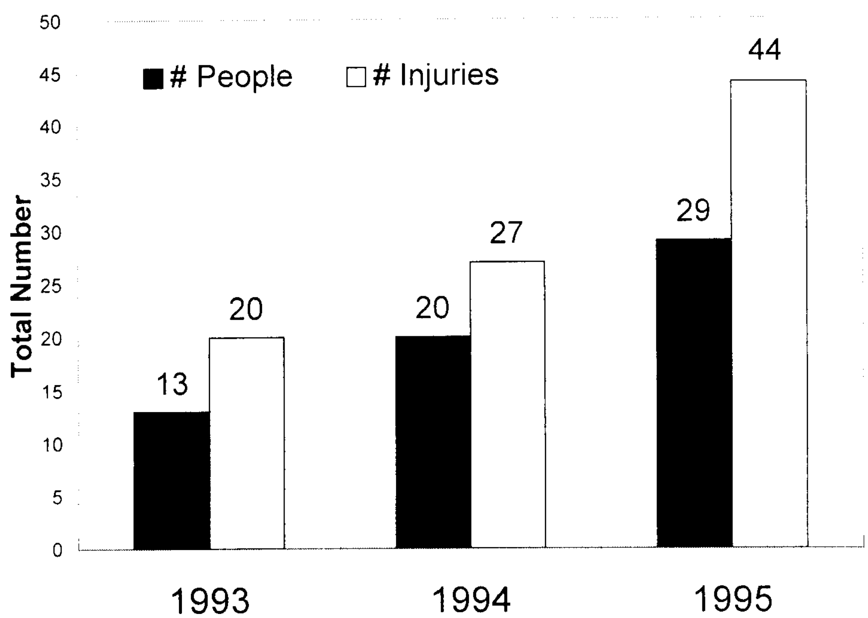

Figure 2: Unweighted Number of People with Airbag-Induced Eye Injuries and the Total Number of Reported Eye Injuries (NASS Files for 1993-1995)

INSTRUMENTED DUMMY HEAD TESTING

EXPERIMENTAL DESIGN - An instrumented Hybrid III dummy head, with the vinyl cover removed, was hit with seven different types of airbags from a pneumatic deployment system. Seven individual force transducers (piezo resistance, 245 N maximum, 0-1 Hz, NipponDenso) were used on the right ocular region and labeled as shown in Figure 3. Each sensor had a contact area of 2.25 cm^2. Only one side of the dummy head was used given the assumed symmetry of the deployment. Each signal was controlled by an individual amplifier and recorded on an eight channel digital tape player. The eighth channel was used to record the airbag's internal pressure from a pressure transducer located on the airbag side of the manifold. An apparatus with six degrees of freedom (X,Y,Z, and 3 rotations) was designed to mount the head in the proper position. This allowed for any modification to the positioning. For these tests, the center of the eye was positioned 12.5 cm above and 15.0 cm away from the center of the airbag as detailed in Figure 4. Preliminary experiments revealed this location to be that of the highest velocity for the deployment system. The head was rigidly mounted to a cart which possessed four wheels that were free to roll on two rails. This allowed the head and cart system to roll away from the airbag after impact.

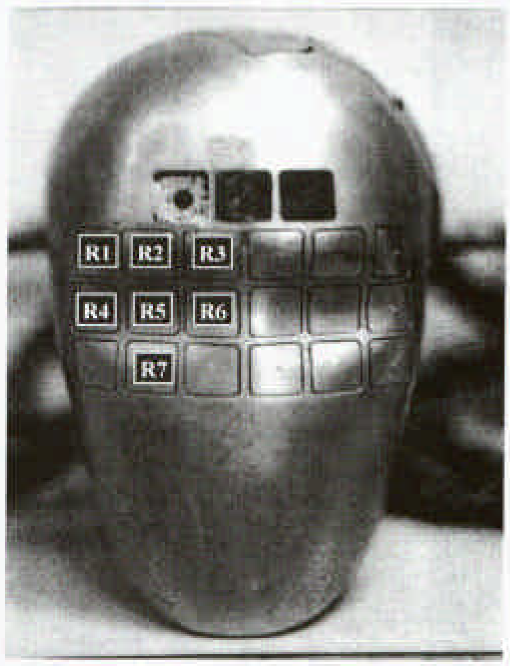

Figure 3: Front View of the Instrumented Dummy Head Showing the Force Transducers Locations and Labeling Pattern

The airbags were deployed via a pressure vessel system. A piston is used for the valve which controls the deployments by a remote set of solenoids and relays. The air pressure in the tank is provided by an air compressor that has a maximum pressure of 0.96 MPa. It is capable of deploying airbags at approximately 60 m/s, which is just below the industry average of 64.5 m/s (22).

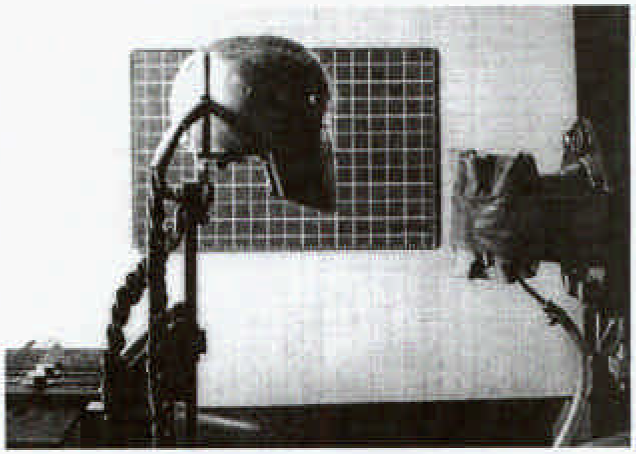

Figure 4: Mounting Position for the Instrumented Dummy Head Relative to the Deployment System

Table 2 details how each airbag type varied for both the instrumented dummy head and cadaver tests, which differed in the material, coating, presence of a tether, and folding pattern. Three separate bags of types 1, 2, 4, 5, 6, and 7, as well as nine bags of type 3 were used for the instrumented dummy head tests giving a total of 27 deployments. Types 3B, 4B, and 5B were used for the cadaver tests as detailed later. The material types and coatings represent proprietary data and are labeled to protect this information.

Table 2: Airbag Construction Specifications

Airbag Type	Material Type	Coating Type	Tether/ Non-tether	Folding Pattern
1	A	A	N	Modified Accordion
2	B	B	N	Modified Accordion
3	B	B	T	Modified Accordion
3B	B	B	N	Accordion
4	B	none	N	Modified Accordion
4B	B	none	N	Accordion
5	B	none	T	Modified Accordion
5B	B	none	T	Accordion
6	C	none	N	Modified Accordion
7	D	none	N	Modified Accordion

RESULTS - The maximum force at each sensor was recorded along with the airbag's maximum internal pressure as noted in Table 3 (located in the Appendix). All recorded data presented is unfiltered. Tests 1 - 21 were run at full pressure while tests 22 - 24 were run at a lower pressure in order to provide a comparison. The maximum force values at each sensor for the full pressure deployments were averaged and are shown in Figure 5. From this chart it can be seen that R2 (upper center of the eye) experiences the highest average force of 63.6 N with R5 (center of the eye) recording the lowest average value of 15.4 N. Given the contact area of 2.25 cm^2 per gauge, the minimum and maximum pressures were 68 kPa and 282 kPa respectively. Using the standard t-test ($p=0.05$), all comparisons, either greater than or less than, of these average values are statistically significant except for R4 vs. R6, and R1 vs. R8. This distribution seems inherently predictable given that the anatomical structure of the orbital region is intended to absorb impact and protect the eye. Furthermore, the dummy head modeled this anatomical configuration with slightly recessed ocular regions.

39 (14)	64 (24)	48 (13)
19 (6)	15 (5)	20 (8)
nr*	32 (5)	nr

Figure 5: Average Maximum Force in Newtons by Sensor for Full Pressure Deployments of the Right Side, Standard Deviation in Parentheses. (*nr = not recorded)

The difference between tethered airbags and nontethered airbags were examined using the resulting forces. Airbags 3 and 5 had tethers while 1, 2, 4, 6, and 7 did not. Figure 6 depicts the average maximum force per sensor for the tethered bags compared to the average maximum force per sensor from the nontethered airbags. A statistical comparison of these averages failed to reject the null hypothesis ($p=0.05$), and therefore shows no significant difference among the recorded forces for tethered versus nontethered airbags. Given the fixed distance of 15 cm between the sensors and the airbag, this similarity in the forces seems appropriate. At this location the effects of the tethering device are not yet noticeable. Figure 6 also reaffirms the force distribution pattern with R2 being the highest and R5 the lowest for both types of airbags.

The effect that maximum internal pressure has on the total force exerted on the ocular sensors was examined in Figure 7. In order to better represent this effect, the total force on the entire ocular region was computed. This was done by first averaging the maximum forces for the three deployments of each airbag type at each sensor. Next, these averages were summed for that airbag. Finally, the three maximum internal pressures for each airbag type were averaged and plotted inside the total ocular force for each airbag type. It is obvious that as the maximum internal pressure drops off in airbag types 4 and 5, the total maximum force stays consistent. Other factors enter into this analysis such as the presence of a coating in airbags 1, 2, and 3, which most likely accounts for the higher internal pressures.

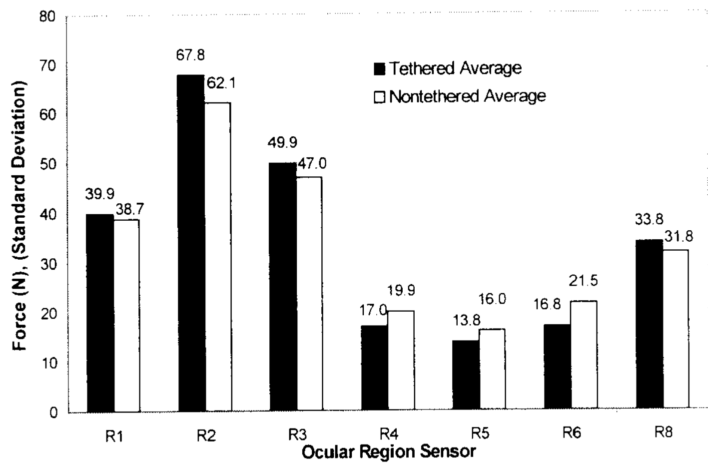

Figure 6: Average Maximum Forces per Sensor for Tethered Versus Nontethered Airbags.

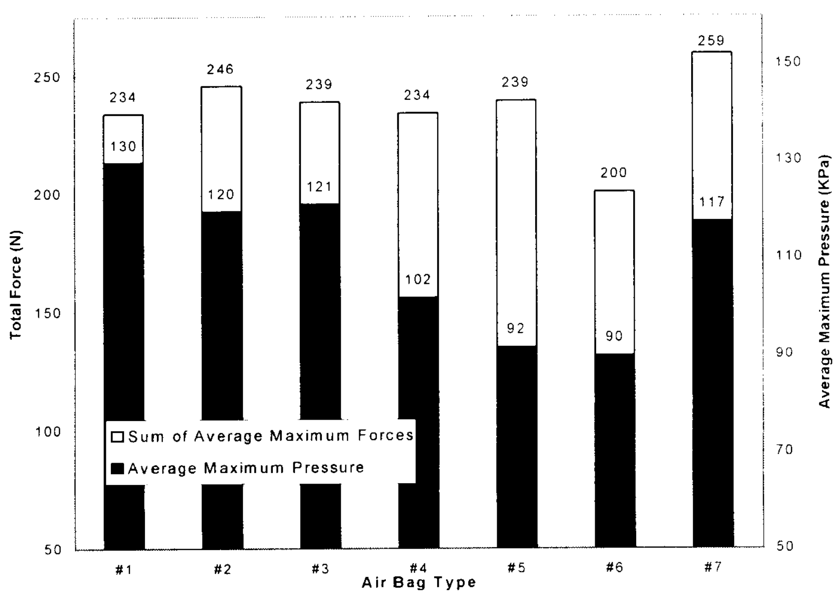

Figure 7: Sum of the Average Maximum Ocular Forces Per Airbag Compared to the Average Maximum Internal Pressure for Full Pressure Deployments

CADAVERIC HEAD TESTING

EXPERIMENTAL DESIGN - Thirteen unembalmed, previously frozen human cadaver heads were impacted with airbags using the deployment system. The testing conditions, as well as the results, are detailed in Table 4. Each test was run with the pressure vessel of the deployment system pressurized to its maximum 0.96 MPa. Since many drivers require eyeglasses, the last four tests were given the special condition of wearing eyeglasses.

Examination Techniques - For biomechanical testing with human cadaver tissue, a critical component is the determination of damage by post-test analyses. Due to the nature of post-mortem tissue, the human cadaver eye presents a particularly difficult area in which to assess trauma. Initial indications of ocular injury in the living almost always manifest as a functional deficit. Such deficits are basically impossible to detect in cadaveric specimens for a number of reasons. Therefore, researchers must carefully note pre-test and post-test anatomy in order to determine damage resulting from a particular biomechanical test.

Surface abrasions and lacerations of the cornea may be made more obvious by the use of a fluorescein dye. This orange dye binds to ulcerated, or excavated, areas of the cornea or sclera. In the presence of cobalt blue light, the damaged areas shine yellow-green. Also, an ophthalmic ultrasound device can be used to evaluate the cadaver eyes. It is very inexpensive (about the same order as X-rays) and the machines are portable. A clear advantage of ultrasound is the fact that images are produced in real time and thus the examination is dynamic. The probe can be manipulated to literally search an area for problems. The basic principle behind ultrasonography is simple sound mechanics. Sound waves are pulsed into an area and the echoes are received and modified. The frequency used for orbital examination is generally 8-10 MHz, while abdomeno-pelvic examinations for fetal development and the like are performed at 1-5 MHz (lower frequency produces longer wavelengths and thus deeper penetration). Ultrasound can be recorded in one dimensional A-mode or two dimensional scanning B-mode. Although the image is much less distinct than that of an MRI, the posterior portions of the eyeball can be examined rather thoroughly. A detached retina is easily diagnosed with a B-mode ultrasound scan.

Procedure - The first head had an intact brain, whereas the brains in tests 2 through 13 had been removed. Five hours were needed before each test to thaw the head completely. Once thawed, the eyelids were removed from the specimens to ensure maximum exposure during testing. This removal process also eliminated the need to fix the eyelids in an open position. In order to solve the problem of low intraocular pressure that is present in postmortem eyes, a 30 gauge needle was used to inject approximately 5 ml of saline into the vitreous until the cornea regained its natural shape. The heads were then put through a series of tests to provide initial data on the eyes before impacting them with the airbag. First, an ophthalmic ultrasound was used to examine the eyes for detached retinas and other abnormalities. The ultrasound image for each eye was recorded with a Polaroid camera. For comparison, several images were taken of healthy live eyes. The last pre-test data included a fluorescein test of both eyes to look for corneal abrasions that may be present before actual airbag impact.

After the initial screening was done, the head was mounted on the cart system at the indicated height (12.5 cm) and distance (15.0 cm) from the center of the airbag. Tests 1 through 9 were mounted as shown in Figure 8, and the experiments with glasses were mounted as seen in Figure 9. A strap and hook system was designed and fastened over the head to keep it in place both during and after impact. High speed film recorded the events at 3000 frames/second, while high speed video recorded them at 2000 frames/second.

Figure 8: Mounting Configuration for Tests 1 Through 9 Without Eyeglasses

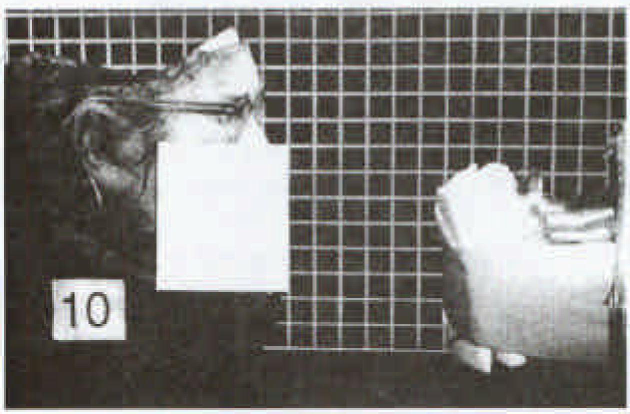

Figure 9: Mounting Configuration for Tests 10 - 13 With Eyeglasses

After each test, ultrasound images were recorded for each eye as well as fluorescein strip test data. The final procedure was to remove both eyes and preserve them for storage using a 30% Formalin solution. Subsequently, they were transported to an ophthalmic pathologist for dissection and examination for abnormalities that may have been related to the impact.

RESULTS - The results for the cadaver tests are shown in Table 4 (located in the Appendix). The impact velocity was taken at the eye from the digitized film. They ranged from the low of 30 m/s to the high of 66 m/s, with the low velocity being the only test with a velocity below 43 m/s. These velocities are below the average maximum leading edge velocity for the industry, but fast enough to provide valid data.

The fluorescein tests revealed damage to the cornea before the deployment with no significant change after impact. This gave the appearance of injury, but was actually due to the fluorescein reacting with the dead cells. The ultrasound images revealed similar results. Figure 10 explains the ultrasound image of a healthy normal eye, while Figure 11 shows one of the cadaver eyes before impact with the airbag. Note the "lack" of material in Figure 10, or the healthy eye; however, in the cadaver eye of Figure 11, it is obvious by the white material in the eye that the retina has detached due to postmortem tissue decay. In fact, all thirteen of the heads used contained eyes that contained detached retinas. Figure 12 shows the same eye as in Figure 11 after airbag impact. From these experiments it can be determined that the retina detaches from the sclera after death. Tests 5, 8, and 10 involved cadaver skin that had decomposed enough to render the outer layer of skin easily separable from the face. In these cases the airbag caused the appearance of inducing an abrasion, but it was due to the dead skin being "brushed" off.

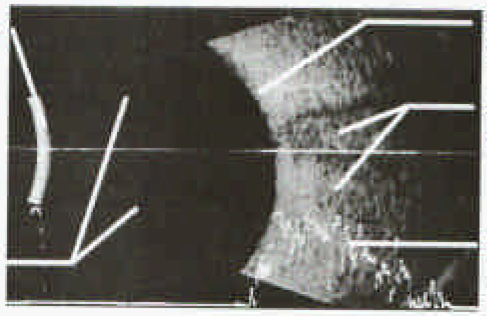

Figure 10: Both A-mode and B-mode Ultrasound Image of Normal Eye with Descriptions of Relevant Anatomy

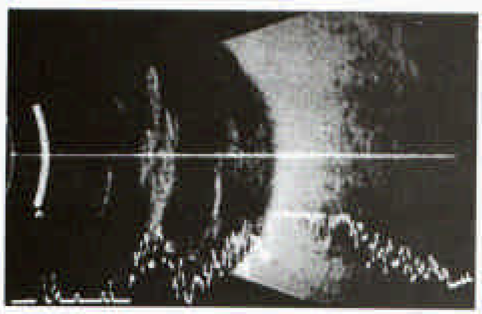

Figure 11: Ultrasound Image of Test 7 Right Eye Before Impact

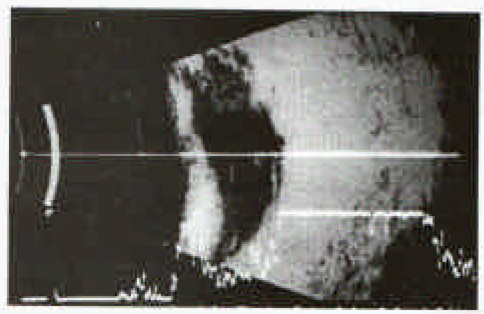

Figure 12: Ultrasound Image of Test 7 Right Eye After Impact

The experiments involving eyeglasses revealed several observations. First, as with the other cases, no injury was noted in any of the four cases involving eyeglasses. Secondly, in test 11 the right lens of the eyeglasses separated from the frames and remained directly over the right eye during impact appearing to "protect" the eye. Test 13 involved common sunglasses that were labeled "impact resistant' in the advertising literature. In this test both lenses separated from the frames, and the frames themselves fractured during the impact, but again no injury was recorded.

The dissection of the eyes confirmed the postmortem detached retinas. Additionally, subluxed lenses, i.e. the lens was displaced from its normal position, were seen in all of the eyes tested. However, this displacement was also viewed as a result of postmortem tissue decay. All of the data suggests no recordable injury from the airbag impacts.

CONCLUSIONS

The combination of cadaver head testing with the instrumented dummy head testing provided many insights into airbag induced eye injuries. The average maximum forces per sensor range from 15.4 N to 63.6 N, with the peak pressures ranging from 68 kPa to 282 kPa. These values are below 3.4 MPa, the lowest ultimate tensile strength Yamada suggests for any ocular tissue, and correspond to the lack of injury recorded in the cadaver tests. The total force for this configuration is independent of airbag material, coating, or presence of a tether. The fact that the forces are approximately the same is most likely due to the small separation distance of only 15 cm for these tests. Within this distance, both tethered and nontethered airbags will appear the same; however, the tether's advantage is in its shorter deployment distance which is more noticeable at full deployment. For this reason airbags with tethers are recommended.

The upper center of the ocular region consistently recorded the highest force values while the center of the region recorded the lowest. Again, this is a logical and protective result of the recessed eye.

It is still unclear exactly what factor eyeglasses play in airbag induced eye injuries. While several case reports indicate injury from broken glasses, tests 10, 11, 12, and 13 for the cadaver heads yielded no injury. In fact, it appears as if the proper "safety eyeglasses," or specially designed glasses that meet impact standards, may be helpful in protecting the eye. As in test 11, the "safety eyeglasses" remained intact and essentially shielded the eye from the airbag.

With a maximum impact velocity of 66 m/s, there were no recordable injuries. This implies that eye injuries occur as a result of airbag impact at higher velocities, but it should be noted that the lack of injury may be due in part to the problematic cadaver tissue.

As with any new experimental procedure, much also was learned about the new technique, and in this study it was the use of human cadaver eyes as a test specimen for airbag impact. Cadaver eyes do provide an accurate structural model in that it is an anatomically correct model of the eye and orbit; however, the tissue response of cadaveric tissue is quite problematic. First, all physiologic analyses of injury are basically useless in cadaveric tissue. Most of the basic ocular examination techniques involve determination of the functional integrity of the visual system. Visual acuity, astigmatism, clarity, visual field and depth of field perception, color perception, pupillary response, and extraocular muscle function simply cannot be determined in dead tissue. Also, the specimen has no blood pressure and therefore bleeding or hemorrhaging is not likely to occur. Although the pressurization of the thoracic regions of cadavers can be effective, this procedure would be ineffective in the eye given the eye's minute vasculature. Shortly after death, the cornea, lens and intraocular fluids (vitreous and aqueous humors) begin to cloud. This renders gross observational, ophthalmoscopic, and slit lamp examinations unproductive in cadaver eyes.

Provided normal intraocular pressure can be re-established, external ocular structures can be studied with reasonable confidence. Orbital fracture thresholds for cadavers are likely to be very similar to those of the living. Provided the decomposition is not advanced, a saline or glycerin injected cadaver eyeball is a relatively good model with which to study corneal and scleral abrasions and lacerations. Clearly, the retina is too fragile to be of value in cadaveric studies as it detaches spontaneously some time shortly after death. A problem that may only be avoided by testing tissue samples from animals extremely close to the time of death.

REFERENCES

1. Augenstein, J.S., Digges, K.H., Perdeck, E.B., et al, "Injuries Sustained by Airbag Protected Drivers," 960660, Society of Automotive Engineers, 1996.

2. Malliaris, A.C., DeBlois, J.H., Digges, K.H., "Airbag Field Performance and Injury Patterns," 960659, Society of Automotive Engineers, 1996.

3. Duma, S.M., Kress, T.A., Porta, D.J., et al, "Airbag-Induced Eye Injuries: A Report of 25 Cases," The Journal of Trauma, Vol. 41, No. 1, p 114, 1996.

4. Onwuzuruigbo, C.J., Fulda, G.J., Larned, D., et al, "Traumatic Blindness After Air Bag Deployment: Bilateral Lenticular Dislocation," The Journal of Trauma, Vol. 40, No. 2, p 314, 1996.

5. Campbell, J.K., "Automobile Air Bag Eye Injuries," Nebraska Medical Journal, Vol. 33, p 306, 1993

6. Huelke, D.F., Moore, J.L., Ostrom, M., " Air Bag Injuries and Occupant Protection," Journal of Trauma, Vol. 3, p 894, 1992.

7. Kuhn, F., Morris, R., Witherspoon, C.D., "Ocular Injuries in Motor Vehicle Crashes," Ophthalmology, Vol. 100, p 1280, 1993.

8. Larkin, G.L., "Airbag-mediated Corneal Injury," American Journal of Emergency Medicine, Vol. 9, p 444, 1991.

9. Lesher, M.P., Durrie, D.S., Stiles, M.C., "Corneal Edema, Hyphema, and Angle Recession After Air Bag Inflation," Archives of Ophthalmology, Vol. 111, p 1320, 1993.

10. Mishler, K.E., "Hyphema Caused by Air Bag," Archives of Ophthalmology, Vol. 109, p 1635, 1991

11. Rosenblatt, M.A., Freilich, B.F., Krisch, D., "Air Bag-associated Ocular Injury," Archives of Ophthalmology, Vol. 111, 1318, 1993.

12. Scott, I.U., John, G.R., Stark, W.J., et al, "Airbag-associated Ocular Injury and Periorbital Fractures," Archives of Ophthalmology, Vol. 111, p 25, 1993.

13. Whitacre, M.M., Pichard, W.A., "Air Bag Injury Producing Retinal Dialysis and Detachment," Archives of Ophthalmology, Vol. 111, p 1320, 1993.

14. Giovinazzo, V.J., "The Ocular Sequelae of Blunt Trauma," Advances in Ophthalmic Plastic Reconstructive Surgery, Vol. 6, p 107, 1987.

15. Fukagawa, K., Tsubota, K., Kimura, C., et al, "Corneal Endothelial Cell Loss Induced by Air Bags," Ophthalmology, Vol. 100, p 1819, 1993.

16. Larson, B.C., Kremer, F.B., Eller, A.W., et al, "Quantitated Trauma Following Radial Keratotomy in Rabbits," Ophthalmology, Vol. 90, p 660, 1983.

17. Ingraham, H.J., Perry, H.D., Donnenfeld, E.D., "Air-bag Keratitis," New England Journal of Medicine, Vol. 324, p 1599, 1991.

18. Smally, A.J., Binzer, A., Dolin, S., et al, "Alkaline Chemical Keratitis: Eye Injury from Air bags," Annals of Emergency Medicine, Vol. 21, p 1400, 1992.

19. Swanson-Biearman, B., Mrvos, R., Dean, B.S., et al, "Air Bags: Lifesaving with Toxic Potential," American Journal of Emergency Medicine, Vol. 11, p 38, 1993.

20. Pfister, R.R., "Chemical Injuries of the Eye," Ophthalmology, Vol. 90, p 1246, 1983.

21. Yamada, H., Strength of Biological Materials, Williams & Wilkins Company, Baltimore, 1970.

22. National Highway Traffic Safety Administration, "Air Bag Deployment Characteristics," Springfield, VA, National Technical Information Services, September, 1992.

CONTACT FOR ADDITIONAL INFORMATION

University of Virginia
Automobile Safety Laboratory
1011 Linden Avenue
Charlottesville, VA, 22902
Phone: 804-296-7288
Fax: 804-296-3453

APPENDIX

Table 3: Configuration and Results for Each Instrumented Dummy Head Test

Test (#)	Air Bag Type	Maximum Internal Pressure (KPa)	Maximum Force (Newtons)						
			Sensor Location						
			R1	R2	R3	R4	R5	R6	R8
1	1	126.1	33.5	46.1	43.7	21.5	19.5	37.1	31.5
2	1	134.1	43.2	58.5	29.6	27.1	24.9	29.9	37.6
3	1	129.2	29.2	49.6	45.9	17.9	12.2	28.7	34.4
4	2	120.5	46.7	54.5	45.1	25.8	14.2	17.4	30.0
5	2	121.9	47.6	54.0	39.4	14.9	14.9	20.6	31.1
6	2	116.4	44.6	54.0	53.1	29.4	29.6	37.9	31.8
7	3	110.7	31.2	35.7	29.4	14.7	14.3	29.2	40.1
8	3	114.2	84.7	75.8	51.5	31.9	12.3	9.6	40.6
9	3	111.4	28.5	61.2	46.5	11.6	19.9	18.8	28.7
10	4	121.5	38.3	73.3	49.8	17.2	9.6	13.4	35.2
11	4	93.3	35.9	97.2	65.2	17.9	18.5	18.7	31.3
12	4	90.6	37.6	34.6	40.4	19.3	11.6	14.5	21.9
13	5	92.2	18.0	50.9	43.4	10.8	12.9	16.5	26.3
14	5	92.2	nr*	nr	nr	nr	nr	nr	nr
15	5	90.4	37.0	115.4	78.6	15.9	9.4	10.0	33.1
16	6	92.6	38.3	76.1	44.2	18.6	15.4	10.6	36.0
17	6	87.3	20.3	51.2	33.1	10.0	7.8	13.9	25.5
18	6	nr	nr	nr	nr	nr	nr	nr	nr
19	7	118.1	46.0	120.1	78.7	17.8	15.0	19.1	36.1
20	7	115.4	32.4	41.2	49.3	21.4	19.7	19.9	31.7
21	7	118.3	48.2	58.8	39.8	20.0	11.3	19.9	31.2
22	3	42.2	14.4	35.4	25.6	9.2	3.3	5.1	13.1
23	3	45.1	14.9	38.2	28.0	10.4	8.2	16.5	12.5
24	3	44.1	nr	nr	nr	nr	nr	nr	nr
25	3	119.1	30.4	89.4	14.2	14.5	14.2	18.1	31.2
26	3	118.9	44.7	87.1	57.8	23.5	17.6	19.6	35.6
27	3	117.5	38.2	104.4	67.9	14.0	10.0	27.3	32.0

* *Data not recorded for this test*

Table 4: Summary of Cadaver Head Experiments and Observations Before and After Test

Test (#)	Air Bag Type	Maximum Pressure (kPa)	Impact Velocity (m/s)	Fluorescein Findings		Ultrasound Findings		Comments
				Pre-Test	Post-Test	Pre-Test	Post-Test	
1	1	*nr	nr	**B yellow covered	B yellow covered			No detectable injury
2	4	88.1	66	**L thick yellow line across center; **R cornea yellow covered	L thick yellow line across center; R cornea yellow covered	B detached retina	B detached retina	No detectable injury
3	5	81.2	58	B thick yellow line across center	B thick yellow line across center	B detached retina	B detached retina	No detectable injury
4	4B		30	B yellow covered	B yellow covered	B detached retina	B detached retina	No detectable injury
5	5B	82.1	53	B yellow covered	B yellow covered	B detached retina	B detached retina	No detectable injury
6	2	102.0	46	B yellow covered	B yellow covered	B detached retina	B detached retina	No detectable injury
7	3	100.2	61	B yellow covered	B yellow covered	B detached retina	B detached retina	No detectable injury
8	3B	101.8	43	B yellow covered	B yellow covered	B detached retina	B detached retina	No detectable injury
9	6	84.7	46	B yellow covered	B yellow covered	B detached retina	B detached retina	No detectable injury
10	7	96.5	63	B yellow covered	B yellow covered	B detached retina	B detached retina	Plastic Frames + Glass Lenses; glasses bent slightly, no detectable injury
11	5	82.9	50	B yellow covered	B yellow covered	B detached retina	B detached retina	Metal Frames + Plastic Lenses; Right lens separated from frame, no detectable injury
12	5	81.6	46	B yellow covered	B yellow covered	B detached retina	B detached retina	Safety Plastic Frames + Lenses; no detectable injury
13	5	81.2		B yellow covered	B yellow covered	B detached retina	B detached retina	Common Sunglasses: Both lenses separated from broken frame, no detectable injury

*nr = Not Recorded **(L = Left Eye; R = Right Eye; B = Both Eyes)

DISCUSSION

PAPER: **An Experimental Study of Airbag Induced Eye Injuries**

PRESENTER: Stefan Duma, University of Virginia

QUESTION: Larry Schneider, UMTRI
As I understand it, you didn't see any corneal abrasions. Is that correct?

ANSWER: Correct.

Q: And your distance was about six inches or so, 150 millimeters.

A: Correct.

Q: We did some research on skin abrasions and we found that the injury event from the airbag was actually a very small part of the airbag fabric unfolding and contacting the skin of the individual at a particular point in time. I just wonder if this isn't such a low probability event that's related to one small part of the airbag contacting the eye to cause that abrasion, that you're just not going to see it very often in these kinds of experiments. It's a function of the fold and it's a function of the distance and all those parameters that go into that probability.

A: Well, that's certainly a possibility. The reason we specified that distance is from some of the research that was published, we wanted to look at the maximum velocity that we could attain with this system and that's why that distance was specified but there are a lot of factors that go into it. So, you're correct.

Q: Guy Nusholtz, Chrysler Corporation
I have one question. You had your velocity at 66 meters per second and most airbags, I assume this is driver, most airbags get faster than that.

A: Correct.

Q: How were you measuring the velocity and was this the velocity at contact or was it the actual maximum velocity?

A: Great question. This velocity was the velocity at contact. The film was digitized and advanced and the final step before eye impact was where we got these velocities from.

Q: What framing rate were you using?

A: We had two. We had video at 1,000 frames per second and we had high speed film at 3,000 frames a second.

Q: 3,000 might be a little low.

A: That was our limits.

Q: Thank you.